

### Thermophysical Assessment of Lead Magnesium Alloy at Different Temperatures

N. Panthi, I. B. Bhandari and I. Koirala

*Central Department of Physics, Tribhuvan University, Kirtipur, Nepal.*

**Doi:** <https://doi.org/10.47011/16.2.3>

*Received on: 02/07/2021;*

*Accepted on: 22/08/2021*

---

**Abstract:** The mixing behavior of lead–magnesium liquid alloy is studied using different modeling equations at various temperatures. The quasi-lattice model has been employed to analyze the concentration-dependent thermodynamic and structural properties of lead–magnesium liquid alloy. To validate the model, the obtained theoretical results are compared with experimental results. The viscosity of the alloy has been studied by the Kozlov–Romanov–Petrov equation, the Kaptay equation, and the Budai–Benko–Kaptay model, whereas surface tension has been studied by the Butler equation, statistical mechanical approach, and the Compound formation model. The primary focus of this study is the interaction parameters among the atoms of the alloy. The alloy shows the moderately interacting and ordering nature within the entire concentration of lead. There is reasonable agreement between the theoretical and experimental data at 973K. The study concludes that the alloy depicts ordering tendency and viscosity and surface tension both decrease with increase in temperature.

**Keywords:** Ordering, Complex formation, Asymmetric, Statistical mechanical approach.

## 1. Introduction

The analysis of temperature and composition-dependent thermo physical behavior of alloys is important in metallurgy and many other technologies. Lead is a soft and ductile metal. It is commercially used as an alloy with different metals like magnesium, tin, antimony, calcium, arsenic, etc.

The lead–magnesium alloy has a eutectic temperature of 248.7 °C at 83% of Pb [1]. It shows the asymmetric nature of many thermodynamic properties. Although some experimentalists investigated the thermodynamic properties of alloys near their melting point, the complete thermodynamic data of the alloy at higher temperatures is lacking till now. Hence, our study is mainly focused on the investigation of thermodynamic, structural, transport, and surface properties of the alloy at different temperatures by considering stable complex  $PbMg_2$  [2] through different theoretical modeling equations.

First, the quasi-lattice model [4] is used for the analysis of the thermodynamic properties. Next, the concentration-dependent surface tension and viscosity of the alloy are investigated. These properties are important in metallurgical science because they determine the surface and transport properties of liquid mixtures. Researchers are therefore trying to study these properties by proposing different models [5-16].

In the investigation of surface properties in metallurgical science, significant attention is given to the concentration disparity between the surface and bulk materials of the alloy. This disparity is primarily attributed to variations in surface energy among the alloy's constituent elements. Atoms with lower surface energy tend to reside on the surface [15], while, theoretically, atoms with larger sizes exhibit a greater inclination to remain on the alloy's surface [16].

There is a lack of experimental data on concentration-dependent surface tension and viscosity at 973 K. Therefore, the objective of this study is to conduct a comparative analysis of the viscosity and surface tension of the Pb-Mg liquid alloy. To study the viscosity, we employ three models: the Kozlov–Romanov–Petrov (KRP) equation [8], the Kaptay equation, and the Budai–Benko–Kaptay model [14]. As for the examination of surface tension, the Butler equation [7], statistical mechanical approach [16], and the compound formation model [17] are used.

## 2. Theoretical Formulation

### 2.1 Thermodynamic Functions

Consider a binary alloy composed of elements  $A$  and  $B$  containing  $N_A$  and  $N_B$  number of atoms of each element, respectively. According to our model, there is a chemical complex  $A_xB_y$  where  $x$  and  $y$  are the small integers in such a way that:



Now the grand partition function [4] in terms of energy ‘ $E$ ’ is written as:

$$\Xi = \sum_E Q_A^{N_A}(T) Q_B^{N_B}(T) \times \exp\left[\frac{(\mu_A N_A + \mu_B N_B - E)}{k_B T}\right] \quad (2)$$

where  $Q_j(T)$  is atomic partition function and  $\mu_j$  is chemical potential of the  $j^{\text{th}}$  ( $j = A, B$ ) element,  $k_B$  is the Boltzmann constant and  $T$  is absolute temperature. From Eq. (2), the excess Gibbs free energy can be obtained as:

$$G_M^{XS} = N k_B T \int_0^C Y dc \quad (3)$$

where  $Y$  activity coefficient ratio of atom  $A$  to  $B$  and  $C$  is the concentration of element of the alloy. By solving Eq. (3), we obtain the excess Gibbs free energy as:

$$G_M^{XS} = N[\theta\omega + \theta_{AB}\Delta\omega_{AB} + \theta_{AA}\Delta\omega_{AA} + \theta_{BB}\Delta\omega_{BB}] \quad (4)$$

where  $\theta = C(1 - C)$  and  $\theta_{j,k}$ 's ( $j, k = A, B$ ) are polynomials in concentration ( $C$ ). Its value depends on the values of  $x$  and  $y$ .  $\omega$  is called as interchange energy,  $\Delta\omega_{jk}$  are interaction energy parameters.

For  $A = \text{Pb}$ ,  $B = \text{Mg}$ ,  $x = 1$ ,  $y = 2$  the values of  $\theta_{j,k}$ 's are found to be [16]:

$$\theta_{AB}(C) = \frac{1}{6}C + C^2 - \frac{5}{3}C^3 + \frac{1}{2}C^4 \quad (5.1)$$

$$\theta_{AA}(C) = 0 \quad (5.2)$$

$$\theta_{BB}(C) = -\frac{1}{4}C + \frac{1}{2}C^2 - \frac{1}{4}C^4 \quad (5.3)$$

Gibbs free energy ( $G_M$ ) of complex forming alloy is given by:

$$\begin{aligned} G_M &= G_M^{XS} + G_M^{\text{ideal}} = G_M^{XS} + N k_B T [C \ln C + (1 - C) \ln(1 - C)] \\ &= RT \left[ \theta \frac{\omega}{k_B T} + \theta_{AB} \frac{\Delta\omega_{AB}}{k_B T} + \theta_{AA} \frac{\Delta\omega_{AA}}{k_B T} + \theta_{BB} \frac{\Delta\omega_{BB}}{k_B T} + C \ln C + 1 - C \ln(1 - C) \right] \quad (6) \end{aligned}$$

The model says that when  $x = 1$ , there is no probability for the  $AA$  pair to be part of the complex so that the coefficient ( $\theta_{AA}$ ) of  $\frac{\Delta\omega_{AA}}{k_B T}$  in above Eq. (6) is zero. In the absence complexes,  $\Delta\omega_{jk}$  is zero.

From the standard thermodynamic relation, the heat of mixing of an alloy is given as:

$$\begin{aligned} \frac{H_M}{RT} &= \frac{G_M}{RT} - \left[ \frac{1}{R} \frac{dG_M}{dT} \right]_{C,N,P} = \theta \left[ \frac{\omega}{k_B T} - \frac{1}{k_B} \frac{d\omega}{dT} \right] + \\ &\theta_{AB} \left[ \frac{\Delta\omega_{AB}}{k_B T} - \frac{1}{k_B} \frac{d\Delta\omega_{AB}}{dT} \right] + \theta_{AA} \left[ \frac{\Delta\omega_{AA}}{k_B T} - \frac{1}{k_B} \frac{d\Delta\omega_{AA}}{dT} \right] + \theta_{BB} \left[ \frac{\Delta\omega_{BB}}{k_B T} - \frac{1}{k_B} \frac{d\Delta\omega_{BB}}{dT} \right] \quad (7) \end{aligned}$$

The entropy of mixing is given as:

$$\frac{S_M}{R} = - \left[ \frac{G_M}{RT} - \frac{H_M}{RT} \right] \quad (8)$$

The activity of the elements of an alloy is obtained by the standard thermodynamic relation as:

$$\ln a_j = \frac{G_M}{RT} + \frac{(1-C_j)}{RT} \left[ \frac{\partial G_M}{\partial C_j} \right]_{T,P,N} \quad (9)$$

Solving Eqs. (6) and (9), we get:

$$\ln a_A = \frac{G_M}{RT} + \frac{1-C}{k_B T} \left[ \begin{aligned} &(1 - 2C)\omega + \\ &\theta'_{AB}\Delta\omega_{AB} + \\ &\theta'_{AA}\Delta\omega_{AA} + \\ &\theta'_{BB}\Delta\omega_{BB} \\ &+ \ln \frac{C}{1-C} \end{aligned} \right] \quad (10)$$

$$\ln a_B = \frac{G_M}{RT} - \frac{C}{k_B T} \left[ \begin{aligned} &(1 - 2C)\omega + \\ &\theta'_{AB}\Delta\omega_{AB} + \\ &\theta'_{AA}\Delta\omega_{AA} + \\ &\theta'_{BB}\Delta\omega_{BB} + \ln \frac{C}{1-C} \end{aligned} \right] \quad (11)$$

where  $\theta'_{AB}$ ,  $\theta'_{AA}$  and  $\theta'_{BB}$  are derivatives of  $\theta_{AB}$ ,  $\theta_{AA}$  and  $\theta_{BB}$  with respect to concentration respectively.

## 2.2. Microscopic Structural Functions

The concentration fluctuation in the long wavelength limit ( $S_{CC}(0)$ ) of an alloy is derived from the relation as [18]:

$$S_{CC}(0) = RT \left[ \frac{\partial^2 G_M}{\partial C^2} \right]_{T,P,N}^{-1} \quad (12)$$

The experimental  $S_{CC}(0)$  can be obtained by using experimental activities from the equation below.

$$S_{CC}(0) = C_B a_A \left[ \frac{\partial a_A}{\partial C_A} \right]_{T,P,N}^{-1} = C_A a_B \left[ \frac{\partial a_B}{\partial C_B} \right]_{T,P,N}^{-1} \quad (13)$$

where  $C_A$  ( $= C$ ) and  $C_B$  ( $= 1 - C$ ) are concentrations of elements  $A$  and  $B$ , respectively.

The Warren–Cowley short-range order parameter ( $\alpha_1$ ) is obtained from the concentration fluctuation in long wavelength limit as:

$$\alpha_1 = \frac{L-1}{L(Z-1)+1}, \quad (14)$$

where

$$L = \frac{S_{CC}(0)}{S_{CC}^{id}(0)}. \quad (15)$$

## 2.3. Viscosity

The molten alloy is studied in terms of viscosity to better understand the atomic transport behavior. It is regarded as a crucial property in the field of metallurgy, as it plays a significant role in various industrial processes and natural phenomena. Viscosity is primarily influenced by factors such as the concentration of the liquid alloy, cohesion energy, and molar volume. [21, 22]. In order to study the atomic transport properties of the Pb–Mg alloy, we compute its compositional dependence of viscosity at temperature 973 K. Due to the lack of experimental data, we compare the alloy's viscosity by using three different models: the Kozlov–Romanov–Petrov, the Kaptay equation, and the Budai–Benko–Kaptay model.

### 2.3.1. Kozlov–Romanov–Petrov (KRP) Equation

The Kozlov–Romanov–Petrov (KRP) equation is developed to calculate the cohesion interaction within a liquid alloy in terms of enthalpic effect. By using this equation, we can better understand and model the viscous flow properties of the liquid alloy system [23]. At temperature  $T$ , the equation is given as:

$$\ln \eta = C_A \ln \eta_A + C_B \ln \eta_B - \frac{H_M}{3RT} \quad (16)$$

where,  $\eta$  is the viscosity of the alloy and  $\eta_j$  ( $j = A, B$ ) is the viscosity of elements  $A$  and  $B$  of the alloy, respectively. For the metals, the change in viscosity with change in temperature is given as [24]:

$$\eta_j = \eta_0 \exp\left(\frac{\epsilon}{RT}\right) \quad (17)$$

where  $\eta_0$  and  $\epsilon$  are constants of each metal having units of viscosity and energy per mole, respectively.

### 2.3.2. Kaptay Equation

Kaptay developed an equation to calculate the viscosity of an alloy by considering the theoretical relationship between the cohesive energy and the activation energy of the viscous flow. At temperature  $T$ , the equation is:

$$\eta = \frac{hN_{Av}}{C_A V_A + C_B V_B + V^E} \times \exp\left(\frac{C_A G_A + C_B G_B - \Phi H_M}{RT}\right), \quad (18)$$

where  $h$ ,  $N_{Av}$ ,  $V_j$  ( $j = A, B$ ) are Planck's constant, Avogadro number and molar volume of pure metal, respectively. Similarly,  $V^E$  is excess molar volume of alloy formation,  $G_j$  is activation energy of the viscous flow in pure metals and  $\Phi$  is a constant with value  $(0.155 \pm 0.015)$  [13].

The activation energy of  $J^{\text{th}}$  metal is calculated by the following equation:

$$G_j = RT \ln\left(\frac{\eta_j V_j}{hN_{Av}}\right) \quad (19)$$

### 2.3.3. BBK (Budai–Benko–Kaptay) Model

The BBK model of viscosity for multicomponent alloy at temperature  $T$  is given as:

$$\eta = \tau \{ T (C_A M_A + C_B M_B) \}^{\frac{1}{2}} \times (C_A V_A + C_B V_B + V^E)^{-2/3} \times \exp\left\{ \left( C_A T_{m,A} + C_B T_{m,B} - \frac{H_M}{\chi R} \right) \frac{1}{T} \right\}, \quad (20)$$

where,  $\tau$  and  $\eta$  are constants and their values are  $(1.80 \pm 0.39) \times 10^{-8}$  and  $(2.34 \pm 0.20)$ , respectively, while  $\chi$  is a semi-empirical parameter with a value of 25.4.  $M_j$  and  $T_{m,j}$ , are molar mass and melting temperature of the alloy's elements ( $j = A, B$ ), respectively.

## 2.4 Surface Tension

In metallurgy and industry, the surface tension of liquid alloy or liquid metal is

considered a prime factor for the processing as well as for the production of new materials because it is related to the surface as well as interface in the molten metal process [25-27]. The interfacial motion resulting from surface tension plays a significant role in various industrial phenomena. In particular, the surface and interfacial motion of molten metals play a major role in metallurgical processes, including solidification, casting, and welding [28]. In our work, we try to study the surface tension of Pb – Mg alloy at 973 K by considering three models or equations: the Butler equation, statistical mechanical approach, and the compound formation model.

### 2.4.1. Butler Equation

According to Butler [7] there is a monolayer at the surface of a liquid as a separate phase equilibrium with the bulk phase. The Butler equation for surface tension ( $S$ ) at temperature  $T$  is given as:

$$S = S_j + \frac{RT}{A_j} \ln \frac{C_j^S}{C_j^b} + \frac{G_j^{s,xs} - G_j^{b,xs}}{A_j} \quad (21)$$

where  $S_j$  is the surface tension of pure element at working temperature,  $G_j^{s,xs}$  and  $G_j^{b,xs}$  are partial excess free energy in the surface and bulk of constituent elements of the alloy, respectively, while  $A_j$  is the molar surface area of  $j^{\text{th}}$  component. It is given as [29]:

$$A_j = \delta (V_j)^{2/3} (N_{Av})^{1/3} \quad (22)$$

where  $\delta$  is geometrical constant and is expressed as:

$$\delta = \left( \frac{3\beta_V}{4} \right)^{2/3} \frac{\pi^{1/3}}{\beta_S} \quad (23)$$

where  $\beta_V$  and  $\beta_S$  are volume and surface packing fractions, respectively. The values of packing fractions depend on the structure of crystal of each component of alloy. For liquid metal,  $\beta_V$  and  $\beta_S$  carry the values of 0.65 and 0.906, respectively [29].

### 2.4.2. Statistical Mechanical Approach

It is the concept of layered structure near the interface. It assumes a surface monolayer on the surface, as well as a layer just below the surface layer that bridges the surface monolayer to the bulk solution [30]. It connects the surface tension to thermodynamic properties through activity coefficients ( $\gamma_j$ ) and interchange

energy ( $\omega$ ) among the elements of the alloy. At temperature  $T$ , it is given as:

$$S = S_j + \frac{k_B T}{\sigma} \ln \frac{C_j^S}{\gamma_j C_j} + [p(1 - C_j^S)^2 + q(1 - C_j)^2] \frac{\omega}{\sigma} \quad (24)$$

Where  $\sigma$  is the mean area of the surface per atom,  $p$  and  $q$  are surface coordination fractions and physically depicts the fraction of number of the nearest neighbors of an atom within its own layer and in the adjoining layers, respectively, and are related as  $p + 2q = 1$ .

The mean atomic surface area  $\sigma$  is given by:

$$\sigma = \sum_j C_j \sigma_j \quad (25)$$

The surface area of each component is given as [31]:

$$\sigma_j = 1.012 \left( \frac{V_j}{N_{Av}} \right)^{2/3} \quad (26)$$

### 2.4.3. Compound Formation Model

This model is based on the assumption of compound formation tendency in the liquid alloy. The equation in this model is developed by using the grand partition function as that of the quasi-lattice model. The equation at temperature  $T$  is given below:

$$\begin{aligned} S &= S_A + \frac{K_B T}{\sigma} \ln \frac{C_A^S}{C_A} + \frac{\omega}{\sigma} [p(\varphi^S - \varphi) - q\varphi] + \\ &\quad \frac{\Delta\omega_{AB}}{\sigma} [p(\varphi_{AB}^S - \varphi_{AB}) - q\varphi_{AB}] + \\ &\quad \frac{\Delta\omega_{BB}}{\sigma} [p(\varphi_{BB}^S - \varphi_{BB}) - q\varphi_{BB}] \quad (27) \\ &= S_B + \frac{K_B T}{\sigma} \ln \frac{C_B^S}{C_B} + \frac{\omega}{\sigma} [p(f^S - f) - qf] + \\ &\quad \frac{\Delta\omega_{AB}}{\sigma} [p(f_{AB}^S - f_{AB}) - qf_{AB}] + \\ &\quad \frac{\Delta\omega_{BB}}{\sigma} [p(f_{BB}^S - \varphi_{BB}) - qf_{BB}] \quad (28) \end{aligned}$$

Where  $\varphi$ ,  $f$ ,  $\varphi_{jk}$ , and  $f_{jk}$  are bulk concentration functions. Similarly,  $\varphi^S$ ,  $f^S$ ,  $\varphi_{jk}^S$ , and  $f_{jk}^S$  are surface concentration functions. For  $x = 1$  and  $y = 2$ , the bulk concentration functions are:

$$\varphi = C^2 \quad (29)$$

$$\begin{aligned} \varphi_{AB} &= \frac{1}{6} + 2(1 - C) - 6(1 - C)^2 + \\ &\quad \frac{16}{3}(1 - C)^3 - \frac{3}{2}(1 - C)^4 \quad (30) \end{aligned}$$

$$\begin{aligned} \varphi_{BB} &= -\frac{1}{4} + (1 - C) - \frac{1}{2}(1 - C)^2 + \\ &\quad (1 - C)^3 - \frac{3}{4}(1 - C)^4 \quad (31) \end{aligned}$$

$$f = (1 - C)^2 \quad (32)$$

$$f_{AB} = -(1 - C)^2 + \frac{10}{3}(1 - C)^3 - \frac{3}{2}(1 - C)^4 \quad (33)$$

$$f_{BB} = -\frac{1}{2}(1 - C)^2 + \frac{3}{4}(1 - C)^4 \quad (34)$$

The functions  $\varphi^S$ ,  $f^S$ ,  $\varphi_{jk}^S$  and  $f_{jk}^S$  can be obtained from Eqs. (29) to (34) by replacing bulk concentration  $C$  with surface concentration  $C^S$ .

### 3. Results and Discussion

#### 3.1. Thermodynamic and Structural at 973 K

During the study of the binary Pb – Mg alloy, we assumed complex with  $x = 1$  and  $y = 2$  in the alloy and computed different thermodynamic and structural properties from the quasi-lattice model. The results thus obtained are discussed below.

##### 3.1.1. Thermodynamic Properties

Equations (6), (7), (8), (10), and (11) are used to analyze the thermodynamic properties as discussed below. Initially, the interaction energy parameters are calculated by successive approximation method for different concentrations, of the alloy with experimental values within the concentration range 0.1–0.9 [2] by using Eq. (6). The best values of such parameters are obtained as:

$$\frac{\omega}{k_B T} = -5.779, \quad \frac{\Delta\omega_{AB}}{k_B T} = 2.808,$$

$$\frac{\Delta\omega_{BB}}{k_B T} = -4.984 .$$

The parameters thus optimized have been considered throughout the calculation to make consistency for the study of other mixing properties. The graph of free energy of mixing versus concentration of lead is shown in Fig. 1. The theoretical and experimental values of free energy of mixing are in reasonable agreement. It has been observed that both computed and experimental values are minimum at about 0.4 concentration of Pb. The computed values of free energy of mixing suggest that the alloy Pb – Mg is moderately interacting. Similarly, being asymmetry at concentration 0.5, the alloy can be classified as an irregular alloy.

The chemical activity of components of an alloy provides the knowledge of the deviation of the alloy from its ideal behavior. According to Porter and Easterling, this activity can provide valuable information about the constituents of the alloy, specifically indicating whether they are willing to leave the solution or not [18]. If the activity is high, the atoms show a high tendency to leave the solution and vice versa [32].

Equations (10) and (11) are used for the determination of the chemical activity of the alloy's components.

The observed and theoretical values of chemical activities of each component of the alloy are shown in Fig. 2. There is good agreement between experimental and theoretical values of activities of Pb and Mg in the alloy at 973K at all concentrations of Pb.

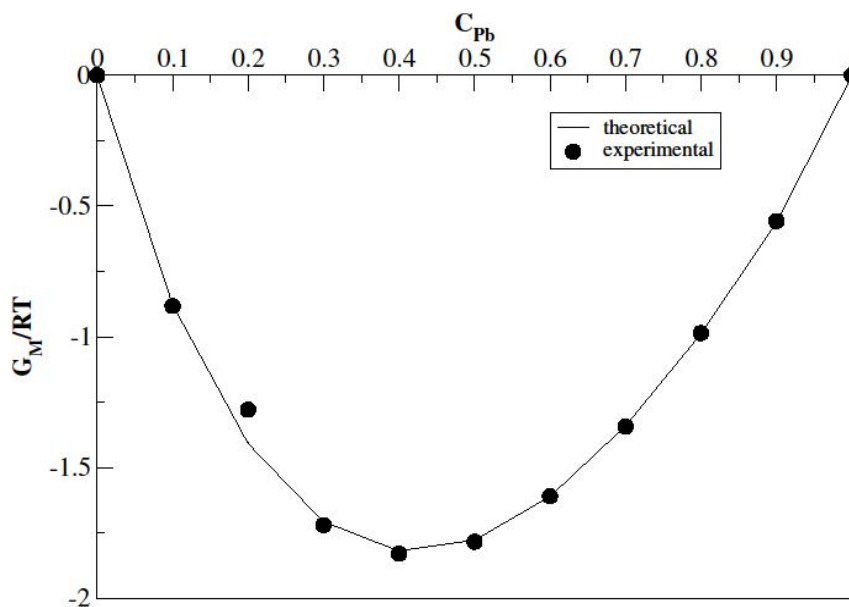


FIG. 1. Gibbs free energy versus concentration of Pb at 973K.

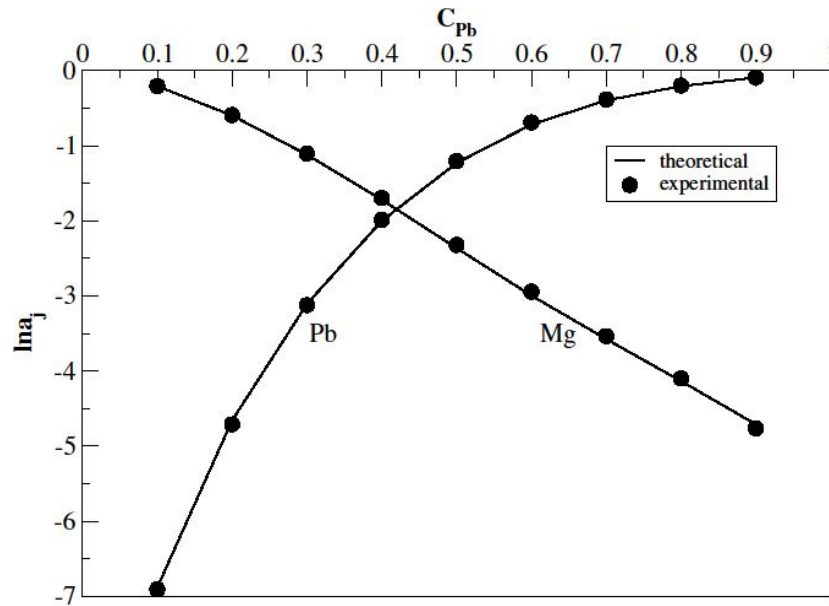


FIG. 2. Chemical activity versus concentration of Pb at 973K.

The theoretical determination of heat of mixing involves obtaining temperature derivatives of the interaction parameters. These parameters are obtained through a process of successive approximation, where a large number of choices are considered. The best-fit values of parameters are:

$$\frac{1}{k_B} \frac{d\omega}{dT} = -0.491, \quad \frac{1}{k_B} \frac{d\Delta\omega_{AB}}{dT} = 1.142,$$

$$\frac{1}{k_B} \frac{d\Delta\omega_{BB}}{dT} = 0.352.$$

The graph of the heat of mixing versus concentration of lead as shown in Fig. 3 depicts that the heat of mixing is more negative at 0.4 concentration of lead. The observed negative heat of mixing suggests that the mixing is

exothermic. The computed and experimental values of  $H_M/RT$  are in reasonable agreement with each other. Using Eqs. (8) and (9), the entropy of mixing ( $S_M$ ) is computed. For theoretical calculation, the energy parameters already obtained during the calculation of Gibbs free energy as well as the heat of mixing of the alloy are used. The plot of entropy of mixing ( $S_M/R$ ) versus concentration of lead is shown in Fig. 4 for both theoretical and observed values. From this figure, it is observed that, despite the minor discrepancy at 0.1 and 0.2 concentrations of lead, the theoretical and experimental values are in agreement with each other in many respects.

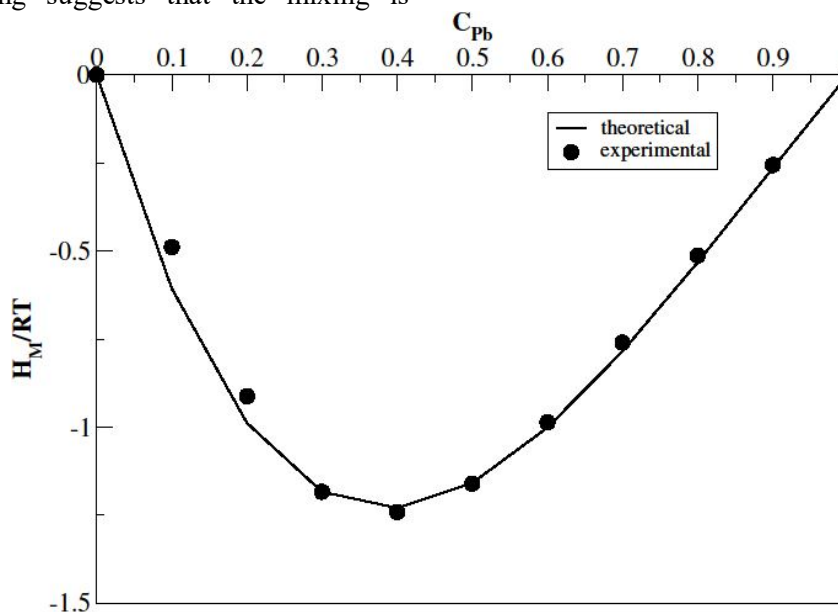


FIG. 3. Heat of mixing versus concentration of Pb at 973K.

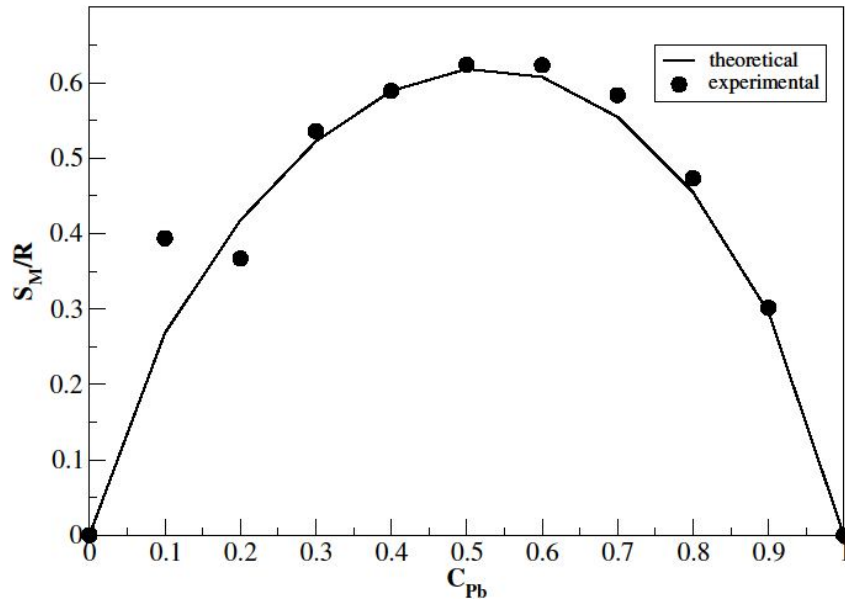


FIG. 4. Entropy of mixing versus concentration of Pb at 973K.

### 3.1.2. Microscopic Properties

In order to study the local arrangement of constituent atoms, the microscopic properties used are concentration fluctuations in the long wavelength limit ( $S_{CC}(0)$ ) and Warren–Cowley short-range order parameter, as these can remove difficulties on the diffraction experiment [18]. The concentration fluctuation in the long-wavelength limit provides information on the local arrangement of atoms, whereas the Warren–Cowley short-range order parameter quantifies the degree of ordering of atoms in the alloys. For a given concentration, if  $S_{CC}(0) < S_{CC}^{id}(0)$ , the expected nature is complex formation and if  $S_{CC}(0) > S_{CC}^{id}(0)$ , the expected nature is segregating. The theoretical and

experimental of  $S_{CC}(0)$  at all concentrations of element lead can be obtained from Eqs. (12) and (13).

The graph of experimental, theoretical, and ideal values of  $S_{CC}(0)$  versus concentration of Pb is shown in Fig. 5. In the graph, the experimental and theoretical values of  $S_{CC}(0)$  are smaller than the ideal value of  $S_{CC}(0)$  at respective concentrations of lead. This indicates the ordering nature of the alloy. The Warren–Cowley short-range order Parameter ( $\alpha_1$ ) is another parameter to quantify the degree of ordering of the liquid alloys. Its value lies between -1 to +1. The negative value shows ordering nature and it is complete for  $\alpha_1 = -1$ .

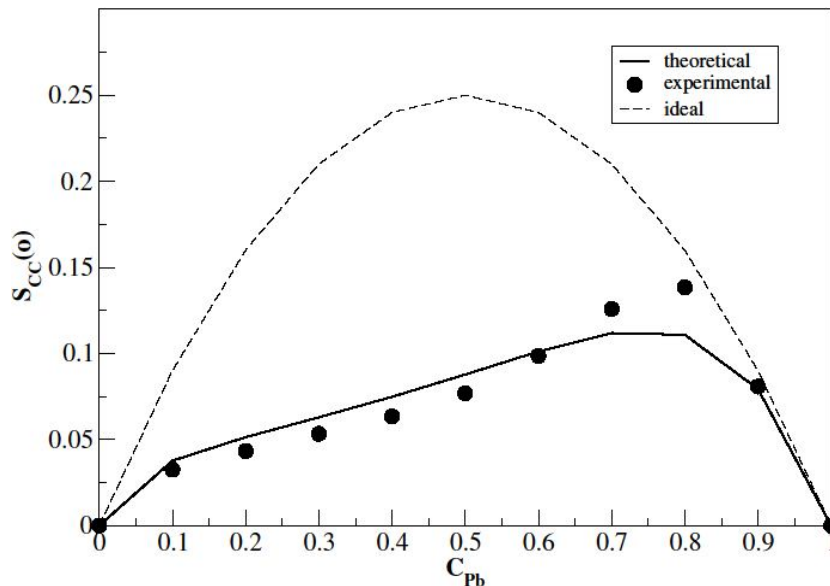


FIG. 5. Concentration fluctuation in long wavelength versus concentration of Pb at 973 K.

. The value  $\alpha_1 = 0$  shows the random distribution of the atoms in the mixture. On the other hand, positive values of  $\alpha_1$  suggest a segregating nature. It is also complete for  $\alpha_1 = 1$ . The graph of theoretical values of  $\alpha_1$  versus concentration of Pb is shown in Fig. (6). The

figure of  $\alpha_1$  is negative within the entire concentration range of lead with the most negative value at 0.2 concentration of lead, signifying strong ordering tendency of the alloy at this concentration.

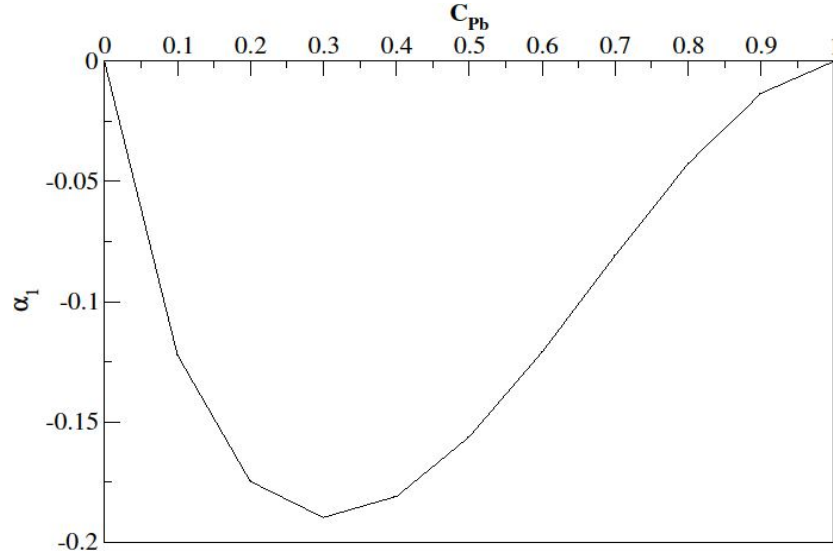


FIG. 6. Warren–Cowley short-range order parameter versus concentration of Pb at 973K.

### 3.1.3 Viscosity

For the theoretical calculation of the viscosity of Pb – Mg alloy at 973 K, the viscosities of each component Pb and Mg at this temperature are required. These values are obtained from Eq. (20) after substituting the values of  $\eta_0$  and E of the metals as given in reference [24]. The value

of enthalpy for different concentrations is used as obtained from Eq. (9) and Gibbs energy of activation of each pure metal is obtained from Eq. (22). As  $V^E$  has no experimental value and the contribution of this term is too small for determination of viscosity of alloy [33], it is considered negligible.

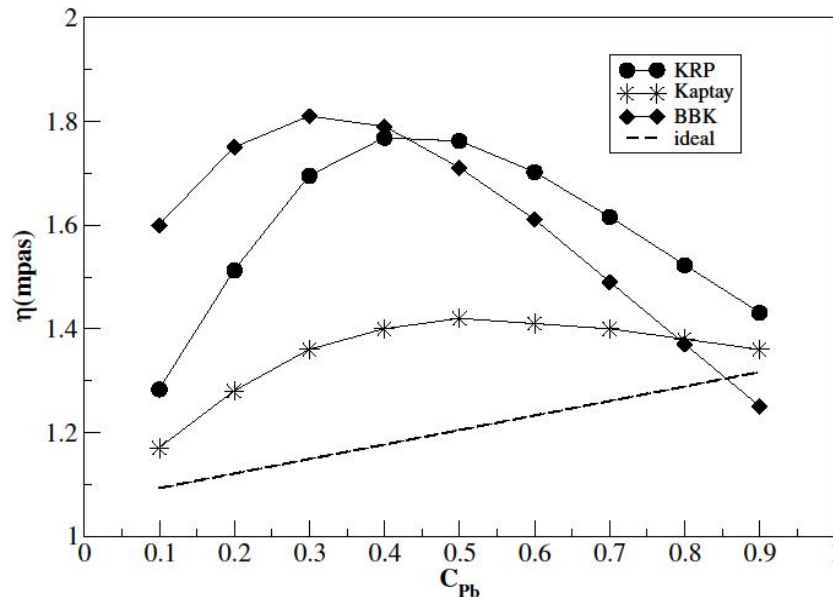


FIG. 7. Viscosity versus concentration of Pb at 973 K.

The results obtained from different models are also compared with the theoretical results of the ideal alloy as shown in the Fig. 7. In all three

models, the viscosity of the liquid alloy at first increases and becomes maximum and then starts to decrease with an increase in the concentration

of the lead. The figure shows that there is a significant deviation of viscosity computed by the BBK and the KRP models within the entire concentration range of lead than that of the Kaptay model, but in this model the value becomes less than the ideal value from 0.8 concentration of the lead. Due to the difference of viscosity of different models and inability of comparison of theoretical results with experimental results, it becomes difficult to draw conclusion regarding the use of the models for the concentration- dependent viscosity of Pb – Mg liquid alloy at temperature 973 K.

### 3.1.4. Surface Tension

To determine the surface tension of the alloy Pb – Mg, we need to find the density and surface tension of individual metals at 973 K, as required by all models. These values are obtained using the relations provided in reference [24]. The bulk and partial excess free energy of individual lead and magnesium at temperature 973K are taken from reference [2]. The values of geometrical structure factor and ratio of surface excess energy to the bulk excess energy ( $G_j^{s,xs} / G_j^{b,xs}$ ) are taken from reference [29]. By utilizing these values in Equation (21) and solving the equations simultaneously, the surface concentrations of both components can be obtained. With the help of these surface concentrations for each respective metal, the surface tension of the alloy is determined. This

procedure is repeated for the other two models, following the same methodology. The interchange energy ( $\omega = -5.779k_B T$ ) as found from Eq. (6) is used in statistical method. Likewise, the interaction energy parameters  $\omega$  and  $\omega_{jk}$  as obtained from the thermodynamic properties are used in the case compound forming model. The surface concentrations and the surface tensions thus computed from all three models are illustrated in Figs. 8 and 9, respectively. From the Fig. 8 it can be concluded that the Pb atoms has segregating tendency to the surface. But such segregating tendency of Pb atoms is more at high bulk concentration of Pb. This also depicts that for concentration of Pb, the lead and magnesium atoms of the alloy interact more and form chemical complexes assumed to be  $PbMg_2$ .

The surface tension of Pb – Mg alloy seems to be decreasing gradually with increasing in bulk concentration of Pb as shown in Fig. 9. But it lies below the ideal value in the statistical mechanical approach after 0.5 concentration of Pb. In the compound formation model, the energy parameters considered are believed to be responsible for the variation of surface tension towards the left side. However, on the right side, complex formation is less likely due to the high surface segregation of lead atoms, as mentioned previously. Hence, the deviation is smaller in this region.

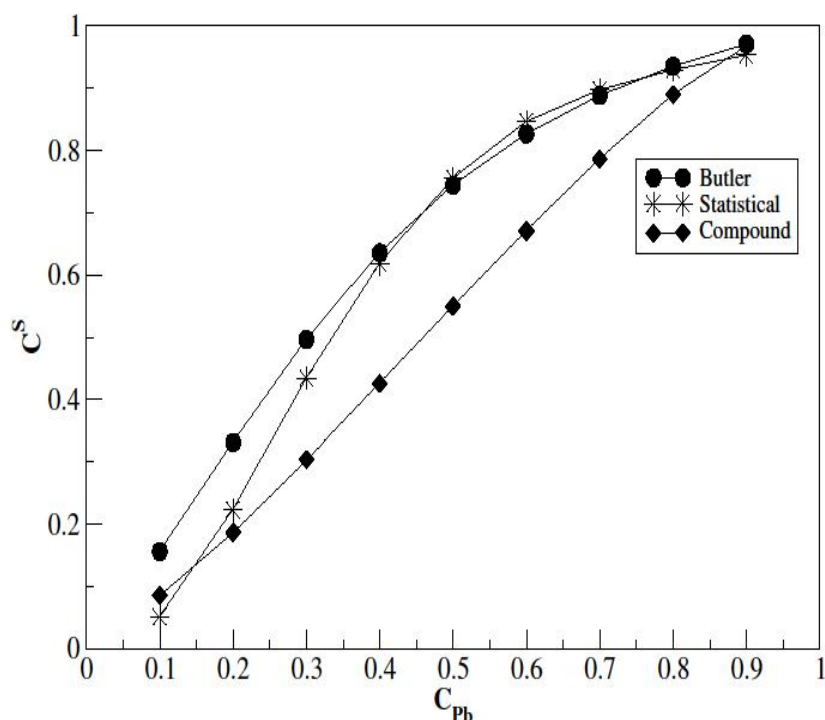


FIG. 8. Surface segregation versus concentration of Pb at 973 K.

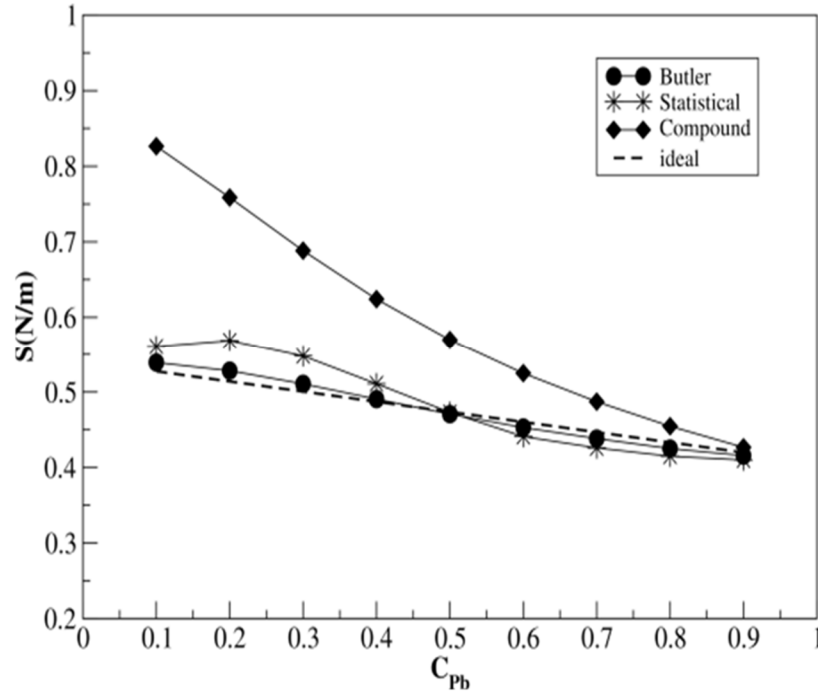


FIG. 9. Surface tension versus concentration of Pb at 973 K.

### 3.2. Thermodynamic, Structural, and Surface Properties at Higher Temperature

For the theoretical analysis of different behavior of the alloy at higher temperatures, we assume that interaction energy parameters linearly depend on temperature and the mole fraction of each component do not depend on temperature. For the theoretical analysis of different behavior of the alloy at higher temperatures, we assume that interaction energy parameters linearly depend on temperature and the mole fraction of each component do not depend on temperature. Based on these assumptions, the change of interaction energy parameter with temperature is expressed as:

$$d[\omega_{jk}(T)]_C = \frac{\partial \omega_{jk}(T)}{\partial T} dT, j \neq k \quad (35)$$

$$\omega_{jk}(T_k) - \omega_{jk}(T) = \frac{\partial \omega_{jk}}{\partial T} (T_k - T) \quad (36)$$

where  $T_k = 1073 \text{ K}, 1173 \text{ K}, 1273 \text{ K}$ .

After solving Eq. (36) by the use of interaction energy parameters and their

temperature derivatives obtained for 973 K, the interaction parameters for different temperatures are found and used in Eq. (6) to compute free energy of mixing for different temperatures. The values thus computed are used for corresponding activities of each component, concentration fluctuation in long wavelength limit, and the compound formation model of surface tension for thermodynamic, structural and surface properties. The plot of Gibbs free energy, activity, concentration fluctuation in long wavelength limit, and surface tension of the alloy at different temperatures are shown in Figs. 10, 11, 12, and 13, respectively.

Figs. 10 and 12 suggest that as temperature increases, the interaction tendency between the atoms decreases so that the alloy becomes less ordered with an increase in temperature. Fig. 11 indicates that each component's activity increases with temperature increase. Whereas Fig. 12 depicts that the surface tension of liquid alloy decreases with an increase in temperature.

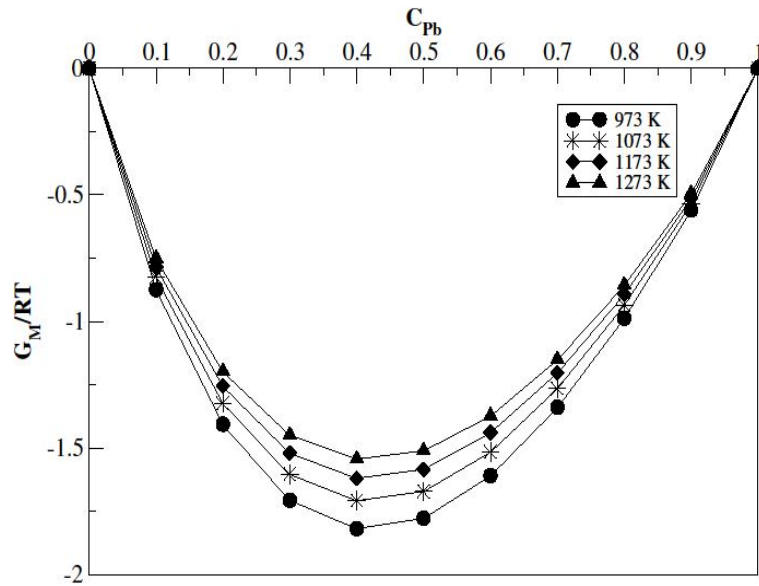


FIG. 10. Gibbs free energy of mixing versus concentration of Pb at different temperatures.

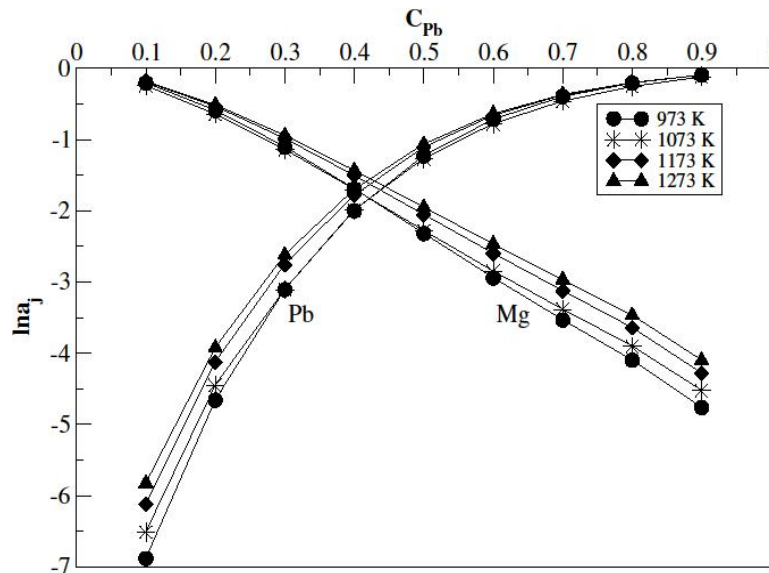


FIG. 11. Chemical activity versus concentration of Pb at different temperatures.

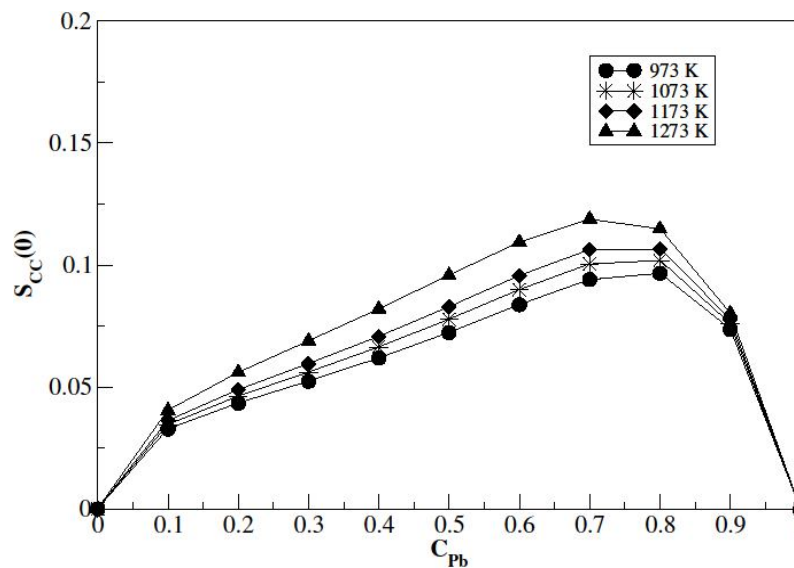


FIG. 12. Concentration fluctuation in long wavelength limit versus concentration of Pb at different temperatures.

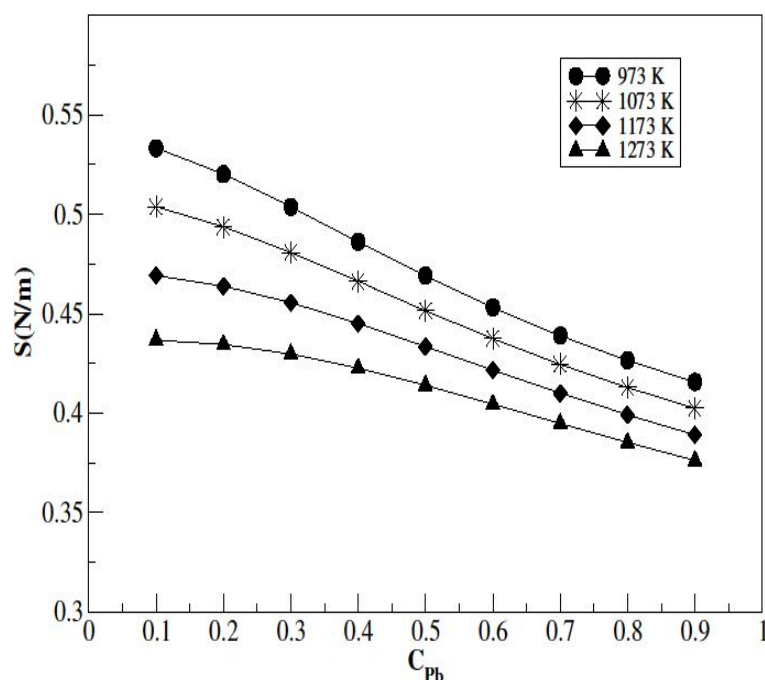


FIG. 13. Surface tension versus concentration of Pb at different temperatures by the compound formation method.

#### 4. Conclusion

In this research paper, theoretical analysis is carried out to understand the thermophysical behavior of binary liquid Pb–Mg alloy at 973 K, 1073 K, 1173 K, and 1273 K by assuming the existence of  $PbMg_2$  complex in the liquid mixture by different models. The paper explains the asymmetric nature of the thermodynamics of the alloy as a function of concentration. This study also shows that the alloy has a tendency of ordering that becomes weaker with an increase in temperature. The study predicts that the lead atoms show a greater tendency to segregate on

the surface at higher concentrations of lead. The viscosity has an erratic variation with an increase in concentration of lead in all models, whereas the surface tension has a nearly linear variation in the Butler and the compound formation models at 973 K. The surface tension decreases with an increase in temperature.

#### Acknowledgements

The authors are grateful to University Grants Commission Nepal for the research grant.

#### References

- [1] Nayeb-Hashemi, A. and Clark, J., Bulletin of Alloy Phase Diagrams, 6 (1985) 56.
- [2] Hultgren, R., Desai, P.D., Hawkins, T., Gleiser, M. and Kelley, K.K., "Selected Values of the Thermodynamic Properties of Binary Alloys", (National Standard Reference Data tem, 1973).
- [3] Okajima, K. and Sakao, H., Transactions of the Japan Institute of Metals, 9 (5) (1968) 325.
- [4] Bhatia, A.B. and Singh, R.N., Physics and Chemistry of Liquids an International Journal, 11 (4) (1982) 343.
- [5] Adhikari, D., Jha, I.S. and Singh, B.P., Philosophical Magazine, 90 (2010) 2678.
- [6] Koirala, I., Journal of Institute of Science and Technology, 22 (2) (2018) 191.
- [7] Butler, J.A.V., Proceedings of the Royal Society A: Mathematical, Physical & Engineering Sciences, 135 (1932) 348.
- [8] Kozlov, L.Y., Romanov, L.M., Petrov, N.N. and Vuzov, I., Chernaya Metall., 3 (1983) 7.
- [9] Iida, T., Ueda, M. and Morita, Z., Tetsu-to-Hagane, 62 (1976) 1169.
- [10] Bhatia, A.B. and March, N.H., Journal of Chemical Physics, 68 (1978) 4651.

- [11] Prasad, L.C. and Singh, R.N., *Physics and Chemistry of Liquids*, 22 (1990) 1.
- [12] Seetharaman, S. and Sichen, D., *Metallurgical and Materials Transactions B*, 25 (1994) 589.
- [13] Kaptay, G., *Zeitschrift Für Metallkunde*, 96 (2005) 24.
- [14] Budai, I., Benko, M.Z. and Kaptay, G., In *Materials Science Forum*, 537 (2007) 489.
- [15] Eldressi, K.A., Eltawahni, H.A., Moradi, M., Twiname, E.R. and Mistler, R.E., "Reference Module in Materials Science and Materials", (Elsevier, 2015).
- [16] Prasad, L.C., Singh, R.N. and Singh, G., *Physics and Chemistry of Liquids*, 27 (1994) 179.
- [17] Novakovic, R., Muolo, M. and Passerone, A., *Surface Science*, 549 (2004) 181.
- [18] Bhatia, A.B. and Thornton, D., *Physical Review B*, 2 (1970) 3004.
- [19] Cowley, J., *Physical Review*, 77 (1950) 669.
- [20] Warren, B.E., "X-ray Diffraction", (Courier Corporation, 1990).
- [21] Poirier, D.R. and Geiger, G.H., "Transport Phenomena in Materials Processing, TMS", (Warrendale, Pennsylvania, USA, 1994).
- [22] Iida, T. and Guthrie, R.I., "The Thermophysical Properties of Metallic Liquids: Fundamentals", (Oxford University Press, USA, 2015).
- [23] Starace, A.K. Neal, C.M., Cao, B., Jarrold, M.F., Aguado, A. and López, J.M., *The Journal of Chemical Physics*, 129 (2008) 144702.
- [24] Brandes, E.A. and Brook, G., "Smithells Metals Reference Book", (Elsevier, 2013).
- [25] Panthi, N., Bhandari, I.B. Jha, I.S. and Koirala, I., *Advanced Material Letters*, 12 (1) (2021).
- [26] Iida, T., *Welding International*, 8 (1994) 766.
- [27] Koirala, I., Singh, B.P. and Jha, I.S., *Scientific World*, 12 (2014) 14.
- [28] Brackbill, U., Kothe, D.B. and Zemach, C., *Journal of Computational Physics*, 100 (1992) 335.
- [29] Kaptay, G., *Materials Science and Engineering: A*, 495 (2008) 19.
- [30] Yeum, K., Speiser, R. and Poirier, D.R., *Metallurgical Transactions B*, 20 (1989) 693.
- [31] Novakovic, R., Ricci, E., Giuranno, D. and Gnecco, F., *Surface Science*, 515 (2-3) (2002) 377.
- [32] Porter, D.A. and Easterling, K.E., "Phase Transformations in Metals and Alloys" (Springer Science + Business Media, B.Y., 1992).
- [33] Jha, I.S., Khadka, R., Koirala, R., Singh, B. and Adhikari, D., *Philosophical Magazine*, 96 (2016) 1664.